THE JOURNAL OF BIOLOGICAL CHEMISTRY
Vol. 275, No. 43, Issue of October 27, pp. 33542–33547, 2000

Printed in U.S.A.

Roles of Individual *N*-Glycans for ATP Potency and Expression of the Rat $P2X_1$ Receptor*

Received for publication, April 6, 2000, and in revised form, August 11, 2000
Published, JBC Papers in Press, August 14, 2000, DOI 10.1074/jbc.M002918200

Jürgen Rettinger‡, Armaz Aschrafi‡, and Günther Schmalzing§¶

From the ‡Department of Pharmacology, Johann Wolfgang Goethe University, Biocenter N 260, Marie-Curie-Strasse 9, D-60439 Frankfurt/Main, Germany and the §Department of Pharmacology and Toxicology, Albert Ludwig University, Hermann-Herder-Strasse, D-79104 Freiburg, Germany

$P2X_1$ receptor subunits assemble in the ER of *Xenopus* oocytes to homotrimers that appear as ATP-gated cation channels at the cell surface. Here we address the extent to which *N*-glycosylation contributes to assembly, surface appearance, and ligand recognition of $P2X_1$ receptors. SDS-polyacrylamide gel electrophoresis (PAGE) analysis of glycan minus mutants carrying Gln instead of Asn at five individual N*X*T/S sequons reveals that Asn^{284} remains unused because of a proline in the +4 position. The four other sites (Asn^{153}, Asn^{184}, Asn^{210}, and Asn^{300}) carry *N*-glycans, but solely Asn^{300} located only eight residues upstream of the predicted reentry loop of $P2X_1$ acquires complex-type carbohydrates. Like parent $P2X_1$, glycan minus mutants migrate as homotrimers when resolved by blue native PAGE. Recording of ATP-gated currents reveals that elimination of Asn^{153} or Asn^{210} diminishes or increases functional expression levels, respectively. In addition, elimination of Asn^{210} causes a 3-fold reduction of the potency for ATP. If three or all four *N*-glycosylation sites are simultaneously eliminated, formation of $P2X_1$ receptors is severely impaired or abolished, respectively. We conclude that at least one *N*-glycan per subunit of either position is absolutely required for the formation of $P2X_1$ receptors and that individual *N*-glycans possess marked positional effects on expression levels (Asn^{154}, Asn^{210}) and ATP potency (Asn^{210}).

The P2X receptor family of ligand-gated cation channels currently comprises seven isoforms ($P2X_1$–$P2X_7$) that are products of seven distinct genes (1–8). The encoded P2X polypeptides bear 36–48% sequence homology. All of the recombinant P2X receptor subunits form functional homomeric complexes when synthesized in heterologous cells. Both biochemical (9) and electrophysiological analyses (10, 11) suggest that trimers represent an essential structural element of P2X receptors, although it must be noted that data consistent with a tetramer have been also obtained (12). P2X receptors open within milliseconds an intrinsic pore nonselectively permeable for small cations when activated by extracellular ATP (for reviews, see Refs. 13–17). During prolonged activation, several P2X receptor channels develop permeability also to rather large cations such as organic dyes (18, 19).

Like virtually all membrane proteins, P2X receptors are glycoproteins. A multitude of functional aspects of oligosaccharides in glycoproteins have been described (for reviews, see Refs. 20 and 21), including influence on topogenesis (22), aid of proper protein folding (chaperone function) (23), quality control in the secretory pathway (24), prevention of marginally stable proteins from unfolding, as well as protein-protein interactions, ligand binding (25), and intracellular trafficking (26). The role of a particular *N*-glycan in a given protein, however, has been found to be rather unpredictable and may comprise several of the above mentioned functions, or it may have no known function at all and be completely dispensable.

The protein sequence of the rat $P2X_1$ subunit shows five putative *N*-glycosylation sites consisting of the N*X*T/S sequon (where *X* denotes any amino acid except proline), which are all located in the predicted $P2X_1$ ectodomain (1). We have recently shown that four of these five putative *N*-glycosylation sites of the rat $P2X_1$ subunit are used in *Xenopus* oocytes (9). Notably, only one of the four *N*-glycans acquires Endo H[1] resistance *en route* to the plasma membrane. Since $P2X_1$ subunits assemble rapidly and quantitatively to noncovalently linked homotrimers soon after synthesis while still in the ER, it seems likely that the three-dimensional structure of the fully assembled and properly folded $P2X_1$ receptor sterically hindered the access of particular Golgi enzymes to three of the four *N*-glycans. Hence, we considered that one or several of these inaccessible *N*-glycans play a role in stabilizing these interactions or even directly participate in subunit interactions in a lectin-like manner.

To examine whether *N*-glycans are important for P2X subunit assembly, surface expression, or ligand recognition, we eliminated *N*-glycosylation sites by site-directed mutagenesis and analyzed the oligomerization and ATP-gated currents of the corresponding receptors in *Xenopus* oocytes by SDS-PAGE, blue native PAGE, and two-electrode voltage clamp measurements, respectively. An additional aim of the study was to examine the effect of *N*-glycans on the migration of P2X receptor complexes in the blue native PAGE system. Our results show that any two out of the four naturally occurring *N*-glycans are sufficient for robust functional expression of $P2X_1$ receptors at the cell surface and that the *N*-glycan in position 210 contributes to ATP potency.

EXPERIMENTAL PROCEDURES

cDNA Constructs—The construction of the His-$P2X_1$ plasmid encoding the rat $P2X_1$ subunit with an N-terminal hexahistidyl tag has been

* The work was supported by grants from the Deutsche Forschungsgemeinschaft (Schm 536/2-1, 536/2-4, and GRK 137/2). The costs of publication of this article were defrayed in part by the payment of page charges. This article must therefore be hereby marked "*advertisement*" in accordance with 18 U.S.C. Section 1734 solely to indicate this fact.

¶ To whom correspondence should be addressed: Institut für Experimentelle und Klinische Pharmakologie und Toxikologie, Hermann-Herder-Str. 5, D-79104 Freiburg, Germany. E-mail: guenther.schmalzing@uni-freiburg.de.

[1] The abbreviations used are: Endo H, endoglycosidase H; ORi, oocyte Ringer's solution; ER, endoplasmic reticulum; PAGE, polyacrylamide gel electrophoresis; NTA, nitrilotriacetic acid; 125*-sulfo-SHPP, ^{125}I-sulfosuccinimidyl-3-(4-hydroxyphenyl)proprionate; DTT, dithiothreitol; PNGase F, peptide:*N*-glycosidase F.

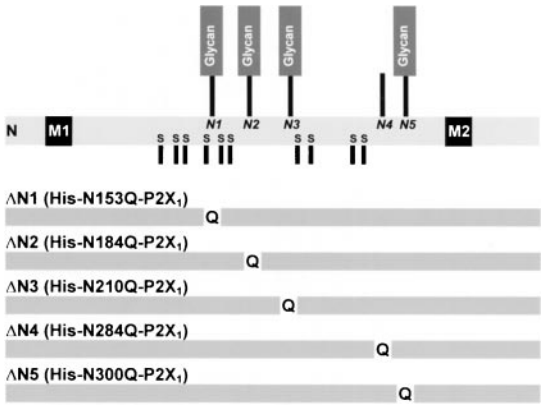

FIG. 1. **Linear model of rat P2X$_1$ showing approximate positions of *N*-glycosylation sequons and corresponding glycan minus mutants.** *N*, cytoplasmic N terminus; *M1* and *M2*, membrane spanning segments; *N1–N5*, asparagine residues of N*X*T/S tripeptides at position 153 (*N1*), 184 (*N2*), 210 (*N3*), 284 (*N4*), and 300 (*N5*). The 10 cysteine residues (*S*), which are conserved among all seven P2X isoforms and which are assumed to form five intramolecular disulfide linkages, are also indicated; an additional conserved cysteine residue (not shown) is located in M2.

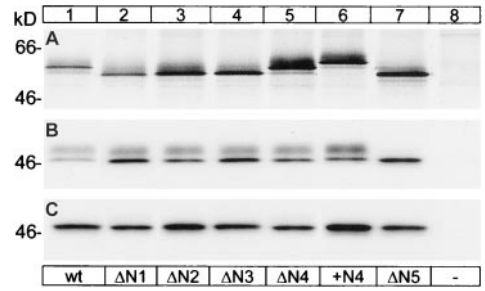

FIG. 2. ***N*-Glycosylation of His-P2X$_1$ mutants each lacking one out of five *N*-glycosylation sites.** Oocytes injected with 23 ng of the indicated cRNAs were metabolically labeled by overnight incubation with [^{35}S]methionine. After an additional 24-h chase interval, digitonin extracts were prepared. Parent His-P2X$_1$ and the various glycan minus mutants were isolated by Ni^{2+}-NTA chromatography, eluted with nondenaturing elution buffer, and then supplemented with SDS sample buffer, 20 mM DTT (final concentration). Samples were incubated for 15 min at 37 °C in the absence (*A*) or for 2 h at 37 °C in the presence of Endo H (*B*) or PNGase F, 1% octyl glucoside (*C*), and then analyzed by SDS-PAGE (10% acrylamide) followed by autoradiography.

described previously (9). His-P2X$_1$ mutants lacking one or several consensus sequences for *N*-glycosylation were generated by changing the Asn of existing N*X*S/T codons to Gln using a commercially available kit (QuikChange™ mutagenesis kit from Stratagene). The resulting His-P2X$_1$ mutants were named ΔN1–ΔN5 (in sequence order) for single mutants (Fig. 1), ΔN12, ΔN13, ΔN15, ΔN23, ΔN25, and ΔN35 for double mutants, ΔN123 and ΔN235 for triple mutants, and ΔN1235 for the quadruple mutant lacking all *N*-glycosylation sites. All mutations were verified by dideoxynucleotide sequencing (27).

cRNA Synthesis—Capped cRNAs were synthesized from *Eco*RI-linearized templates with SP6 RNA polymerase (Amersham Pharmacia Biotech), purified by Sepharose chromatography and phenol-chloroform extraction, and dissolved in 5 mM Tris/HCl, pH 7.2, at 0.5 μg/μl, using the optical density reading at 260 nm for quantitation (OD 1.0 = 40 μg/μl).

Injection and Maintenance of Xenopus oocytes—Xenopus laevis females received from South Africa were anesthetized with MS222 (tricaine) for surgical removal of ovaries. After collagenase treatment (28) defolliculated stage V or VI oocytes were manually selected and injected with 50-nl aliquots of cRNAs. Injected oocytes were kept in parallel with noninjected controls at 19 °C in sterile oocyte Ringer's solution (ORi: 90 mM NaCl, 1 mM KCl, 1 mM $CaCl_2$, 1 mM $MgCl_2$, and 10 mM Hepes, pH 7.4) supplemented with 50 μg/ml of gentamycin.

Radioactive Labeling of Oocytes and Protein Purification—cRNA-injected oocytes and noninjected controls were metabolically labeled by overnight incubation with L-[^{35}S]methionine (>40 TBq/mmol, Amersham Pharmacia Biotech) at about 100 MBq/ml (0.4 MBq per oocyte) in ORi at 19 °C and then chased as indicated. The His-P2X$_1$ receptor and its mutants were purified by Ni^{2+}-NTA-agarose (Qiagen) chromatography from digitonin (1.0%) extracts of oocytes as detailed previously (9). Protein was released from the Ni^{2+}-NTA-agarose with nondenaturing elution buffer consisting of 200 mM imidazole HCl, pH 6.8, and 1.0% digitonin. Eluted proteins were kept at 0 °C until analyzed.

For selective labeling of His-P2X$_1$ receptors at the plasma membrane, oocytes injected with cRNA 3 days earlier were incubated with ^{125}I-sulfosuccinimidyl-3-(4-hydroxyphenyl)proprionate (^{125}I-sulfo-SHPP), a membrane-impermeant derivative of the Bolton-Hunter reagent (29) exactly as described previously (9). Proteins were purified from digitonin extracts of the oocytes by Ni^{2+}-NTA-agarose chromatography as above.

Blue Native PAGE and SDS-PAGE—Blue native PAGE (30, 31) was carried out as described previously (9, 32, 33). Just before gel loading, purified proteins were supplemented with blue native sample buffer to final concentrations of 10% glycerol, 0.2% Serva blue G, and 20 mM sodium 6-amino-*n*-caproate and applied onto polyacrylamide gradient slab gels. Molecular mass markers (Combithek II™, Roche Molecular Biochemicals) were run on both borders of the gel and were visualized by Coomassie Blue staining. For SDS-PAGE, proteins were supplemented with SDS sample buffer containing DTT and electrophoresed in parallel with ^{14}C-labeled molecular mass markers (Rainbow™, Amersham Pharmacia Biotech) on SDS-polyacrylamide gradient gels. When indicated, samples were treated prior to SDS-PAGE with either Endo H or PNGase F (New England Biolabs) in the presence of 1% octyl glucoside to diminish inactivation of PNGase F. Gels were fixed, dried, and exposed at −80 °C to BioMax MR or MS film (Kodak) as appropriate. In some experiments, radioactive bands were quantified with an image analyzer (PhosphorImager 445 SI, Molecular Dynamics).

Two-electrode Voltage Clamp Measurements—Current responses were measured by using the two-electrode voltage clamp technique on oocytes injected with His-P2X$_1$ cRNA 3 days earlier. The electrodes contained 3 M KCl and had resistances of 0.5–2 MΩ. The superfusion solution consisted of 90 mM NaCl, 1 mM KCl, 2 mM $MgCl_2$, and 5 mM Hepes/NaOH, pH 7.4. Calcium salts were omitted to avoid activation of endogenous Ca^{2+}-dependent Cl^- channels. A fast and reproducible solution exchange was achieved as described previously (9). Current signals were elicited by ATP at 1-min intervals, low pass-filtered at 100 Hz, and sampled at 200 Hz using the Turbo TEC-05 amplifier (NPI Electronics, Tamm, Germany). All measurements were performed at room temperature (20–22 °C).

RESULTS

The P2X$_1$ Polypeptide Carries Glycans at Asn^{153}, Asn^{184}, Asn^{210}, Asn^{300}, but Not at Asn^{284}—The P2X$_1$ cDNA has been originally cloned from rat *vas deferens*, where the P2X$_1$ receptor plays a role in muscle contraction (1), which propels sperm into the ejaculate (34). The P2X$_1$ polypeptide chain is 399 amino acids long. For affinity purification after synthesis in *Xenopus* oocytes, we tagged the rat P2X$_1$ polypeptide at its N-terminal end with six histidine residues, which had no effect on ATP-induced currents (9). The His-P2X$_1$ subunit can be isolated from cRNA-injected and [^{35}S]methionine-labeled oocytes as a 57-kDa glycoprotein (Fig. 2*A*, *lane 1*) that carries four *N*-glycans making up ~18% by mass of the protein (9). The deduced amino acid sequence of the P2X$_1$ subunit shows five asparagines for possible *N*-linked glycosylation (N*X*T/S): N^{153}GT, N^{184}FT, N^{210}GT, N^{284}LS, and N^{300}GT. Replacement of Asn^{153}, Asn^{184}, Asn^{210}, and Asn^{300} by Gln, one at a time, resulted in the synthesis of glycoproteins that had a 2–3 kDa lower mass than the wild type P2X$_1$ glycoprotein (Fig. 2*A*, *lanes 2–4* and *7*). Since 2–3 kDa corresponds to the mass of one *N*-linked oligosaccharide side chain, this finding implies that each of the replaced asparagines is occupied by an *N*-glycan in the wild type P2X$_1$ subunit. In contrast, replacement of Asn^{284} by Gln had no effect on the mass (Fig. 2*A*, *lane 5*), indicating that Asn^{284} of the wild type P2X$_1$ subunit is the asparagine that is not used as a glycosyl acceptor site.

The inability to glycosylate Asn^{284} of the N^{284}LS sequon may be attributed to the leucine residue in the *X* position, which has been found to impair core glycosylation (35). Alternatively, Pro^{287} immediately following the N^{284}LS sequon might be re-

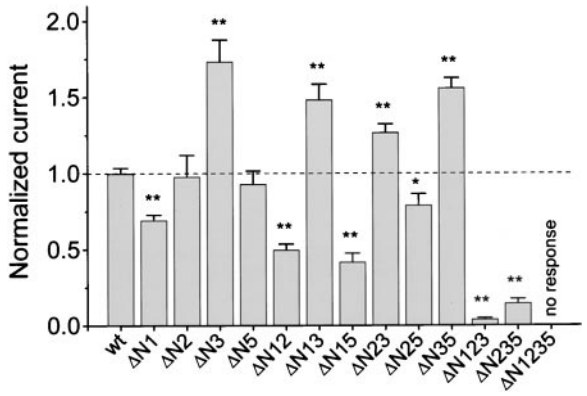

FIG. 3. **Comparison of maximum inward current responses generated by parent P2X$_1$ and glycan minus mutants.** Oocytes were injected with 23 ng of the indicated cRNAs. After 3 days at 19 °C, currents were activated at a holding potential of −40 mV by 30 μM ATP, which elicits maximum responses at parent His-P2X$_1$ and each mutants. Currents were normalized to the response of the parent His-P2X$_1$ receptor. Data are given as means ± S.E. from 20–48 oocytes per column of two to six experiments with 6–10 oocytes per experimental condition. Currents significantly different from that of parent His-P2X$_1$ are denoted by *asterisks* (*, $p < 0.05$; **, $p < 0.001$).

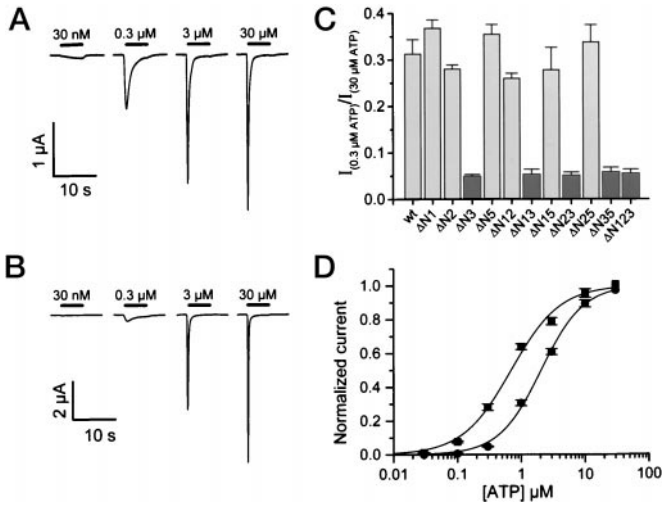

FIG. 4. **Comparison of ATP potency between parent His-P2X$_1$ and glycan minus mutants.** Inward current traces were recorded at the indicated ATP concentrations and a holding potential −40 mV from oocytes injected 3 days earlier with 23 ng of cRNA for parent His-P2X$_1$ (*A*) or the glycan minus mutant ΔN3 (*B*). *C*, the ratio between currents activated at −40 mV by 0.3 and 30 μM ATP was calculated as a measure of the ATP potency at the various glycan minus mutants (n = 5–6, mean ± S.E.). Note that all mutants lacking *N*-glycosylation site N3 exhibit a markedly decreased current ratio indicative of a reduced ATP potency. *D*, ATP dose-response curve for parent His-P2X$_1$ (■) and mutant ΔN3 (●). Currents were elicited by the respective ATP concentration in 1-min intervals. Continuous lines represent least squares fits of the Hill equation to the data points, yielding EC$_{50}$ values of 0.7 ± 0.1 μM (Hill coefficient of 1.1 ± 0.1) and 2.1 ± 0.2 μM (Hill coefficient of 1.3 ± 0.1) for parent His-P2X$_1$ and mutant ΔN3, respectively (n = 6–7, mean ± S.E.).

sponsible, since proline inhibits core glycosylation not only at the *X*, but also at the +4 position (36). Indeed, Asn^{284} was efficiently used as a glycosyl acceptor site when alanine was substituted for Pro^{287}, as inferred from the reduced mobility of the His-Ala^{287}-P2X$_1$ polypeptide, indicating the presence of an additional (fifth) *N*-glycan (Fig. 2*A*, *lane 6*). The occupancy of Asn^{284} by a glycan had no apparent effect on P2X$_1$ receptor function, as deduced from the magnitude and concentration dependence of ATP-gated currents (results not shown). The efficient glycosylation at Asn^{284} after elimination of Pro^{287} argues against a significant role of Leu^{285} for the inability to glycosylate Asn^{284} of the parent P2X$_1$ polypeptide.

Solely the Glycan at Asn^{300} Acquires Complex-type Carbohydrates—From the four *N*-glycans per P2X$_1$ receptor subunit, only one acquired Endo H resistance during transport to the plasma membrane of *Xenopus* oocytes (9). This suggests that processing by Golgi enzymes of three of the *N*-glycans is sterically hindered, most likely as a result of folding and oligomerization of the P2X$_1$ chains. Fig. 2*B* shows that like the parent His-P2X$_1$ receptor (*lane 1*) all the P2X$_1$ receptor mutants (*lanes 2–6*) except ΔN5 (*lane 7*) acquired Endo H-resistant carbohydrates. Since the P2X$_1$ receptor mutant ΔN5 appears at the plasma membrane (*cf.* Figs. 3–5), the absence of Endo H-resistant carbohydrates can be directly conferred to the lack of the sole *N*-glycan that can acquire complex-type carbohydrates during transit of the Golgi apparatus. This indicates that the glycan at Asn^{300} of the parent His-P2X$_1$ receptor subunit is the one accessible for complex glycosylation.

At Least One N-Glycan per Subunit at Either Position Is Needed for P2X$_1$ Receptor Formation—To examine whether the elimination of a particular *N*-glycan affects the expression level of functional P2X$_1$ receptors, we recorded current responses to 30 μM ATP at −40 mV. This ATP concentration elicited different yet maximum responses at the parent P2X$_1$ receptor and all receptor mutants, since activation with 100 μM ATP did not result in a further increase of currents. Like the parent P2X$_1$ receptor, also all receptor mutants lacking one *N*-glycan per subunit exhibited large ATP-gated currents, indicating that no particular *N*-glycan is essential for receptor function (Fig. 3). There are, however, marked positional effects of the *N*-glycans. While the glycans at N2 or N5 were without significant effect on the expression level of functional receptors, elimination of the glycan at N1 or N3 resulted in a 30% decrease or 70% increase, respectively, of the current response (Fig. 3). Likewise, reduced currents were recorded from double mutants that lacked N1 together with N2 or N5, whereas elimination of N3 consistently resulted in increased currents even when N1 was simultaneously eliminated (Fig. 3). These findings suggest that the glycans at N1 and N3 play opposing roles for the expression level of functional P2X$_1$ receptors.

Elimination of any three *N*-glycans did also not prevent P2X$_1$ receptor formation, but the functional expression level decreased markedly to <10% of that of the parent P2X$_1$ receptor. The currents were particularly low when the three acceptor sites that were eliminated included N1 (Fig. 3). No ATP-induced currents could be recorded from oocytes after removal of all canonical *N*-glycosylation sites. Taken together, these results implicate that despite their marked positional effects, only one *N*-glycan at any locus is required for the formation of functional P2X$_1$ receptors, and two such sites are sufficient for robust functional expression.

Elimination of the Glycan at Asn^{210} Decreases ATP Potency—Since *N*-glycans are bulky and can shield a large section of the protein surface, we examined whether elimination of *N*-glycans affects ATP potency. To this end, we recorded receptor currents elicited by 0.3 and 30 μM ATP and determined the ratio of the current responses at these two ATP concentrations. As apparent from Fig. 4*C*, all the receptor mutants lacking N3 (Asn^{210}) showed a current ratio of 5–7% independent of simultaneous elimination of additional *N*-glycosylation sites. In contrast, all glycan minus receptor mutants that contained *N*-glycan N3 showed a ratio of 26–37% similar to the 32% for the parent His-P2X$_1$ receptor. Since N3 turned out to be crucial for the reduced potency, concentration response curves for ATP of ΔN3 and parent His-P2X$_1$ were recorded. Fitting the Hill equation to the data for the parent His-P2X$_1$ receptor yielded an EC$_{50}$ value for ATP of 0.7 μM (Fig. 4*D*). In contrast, the glycan minus

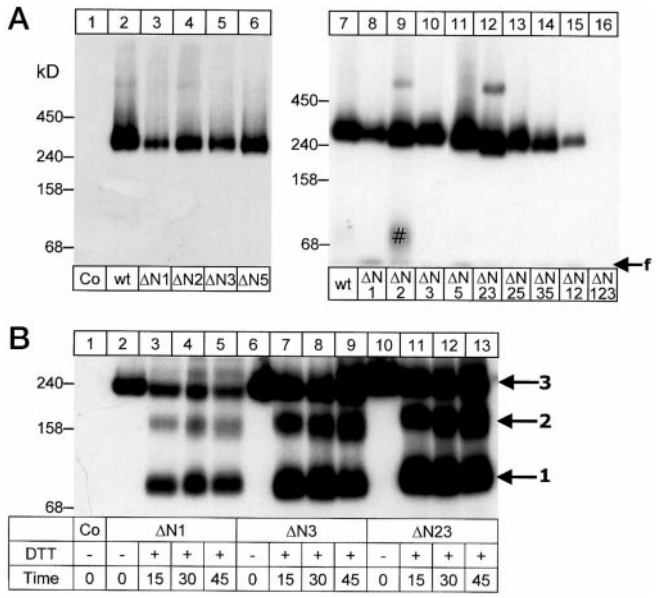

FIG. 5. **Glycan minus mutants migrate as trimers like parent P2X$_1$ when analyzed by blue native PAGE.** Oocytes injected with the indicated cRNA 3 days earlier were surface-labeled with membrane impermeant ^{125}I-sulfo-SHPP and extracted with digitonin. His-P2X$_1$ and the His-tagged mutant proteins were then purified by Ni^{2+}-NTA chromatography under nondenaturing conditions and resolved by PAGE followed by autoradiography. *A*, proteins were resolved immediately after native elution by blue native PAGE (4–10% acrylamide gradient gel). Shown are samples from two independent experiments. #, contaminating protein not observed in other experiments (*cf. lane 4*); *f*, front. *B*, proteins were analyzed after native elution either without further treatment or after incubation with 100 mM DTT for the indicated time period. *Numbered arrows* indicate positions of monomers, dimers, and trimers.

receptor mutant ΔN3 exhibited an EC_{50} value of 2.1 μM, *i.e.* a 3-fold reduced potency for ATP. The Hill coefficients (1.1 *versus* 1.3) were not significantly different.

P2X$_1$ Glycan Minus Receptor Mutants Migrate as Homotrimers When Resolved by Blue Native PAGE—An additional aim of the present study was to examine the influence of carbohydrates on P2X$_1$ receptor assembly as assessed by blue native PAGE analysis. Parent His-P2X$_1$ subunits combine rapidly to stable homotrimers that exit the ER (9), transit the Golgi where complex glycosylation of N5 occurs (Fig. 2), and finally appear at the plasma membrane. To visualize the plasma membrane form of the His-P2X$_1$ glycan minus receptor mutants, we radioiodinated oocyte surface proteins with membrane impermeant ^{125}I-sulfo-SHPP and then isolated the His-tagged proteins by Ni^{2+}-NTA chromatography. When resolved by blue native PAGE, the parent His-P2X$_1$ receptor migrated at 250–290 kDa (Fig. 5) as reported previously (9). Overall, elimination of *N*-glycans resulted in a slight increase in electrophoretic mobility, corresponding maximally to 20 kDa when two *N*-glycans per subunit were lacking (Fig. 5*A*). Within the technical limits of receptor quantification by surface radioiodination, all the receptor mutants lacking one *N*-glycan (Fig. 5*A*, *lanes 3–6* and *8–11*) and most of the mutants lacking two *N*-glycans (*lanes 12–14*) were present at approximately the same density at the plasma membrane as the parent His-P2X$_1$ receptor. The amount of receptor protein decreased markedly when the two acceptor sites that were eliminated included N1 (Fig. 5*A*, *lane 15*) or when three *N*-glycans per subunit were eliminated (*lane 16*). We did not attempt to directly correlate radioiodinated protein and current responses, because differences in the 50% range resolvable by electrophysiological analysis cannot be reproducible detected by surface radioiodination.

To display the oligomeric state of these receptor complexes, we exposed the natively eluted His-P2X$_1$ mutant receptors to DTT in the presence of Coomassie Blue and sodium 6-amino-*n*-caproate. This treatment causes a partial dissociation of the parent His-P2X$_1$ receptor to the monomer and dimer of apparent masses similar to 80 and 170 kDa, respectively, indicating that the nondenatured 250-kDa protein band must be a His-P2X$_1$ homotrimer (9). Likewise, also the His-P2X$_1$ glycan minus receptor mutants lacking one or two *N*-glycans per subunit dissociated into dimers and monomers when exposed to DTT (Fig. 5*B*). Quantification of the bands by phosphor image analysis shows that the extent of dissociation induced by DTT is virtually identical for the three *N*-glycan minus mutant receptors. It should be noted that the dissociating effect of DTT does not result from a cleavage of intersubunit disulfide linkages, but from a perturbation of noncovalent subunit interactions. Dissociation of P2X$_1$ complexes into monomers could also be produced by other denaturing additions such as urea or SDS, which by themselves will not affect disulfide bonds (9). In summary, receptor mutants lacking up to three *N*-glycans per subunit exist in a homotrimeric state like the wild type P2X$_1$ receptor. A mutant that lacked all four *N*-glycans could neither be detected by two-electrode voltage clamp measurements nor by Ni^{2+} chelate chromatography followed by SDS-PAGE and autoradiography.

DISCUSSION

Factors That Control N-Glycosylation of P2X$_1$ Receptors—The P2X$_1$ receptor influences its own *N*-glycosylation at two levels: (i) at the level of its primary sequence and (ii) the level of its three-dimensional structure. First, the N^{284}LS tripeptide (N4) is not used as a site for *N*-glycosylation because of a proline residue in the +4 position. Replacement by alanine resulted in unimpaired *N*-glycosylation at this site. This observation agrees well with previous reports that the presence of proline immediately following a sequon can inhibit core glycosylation (36, 37). A sequon with a proline in +4 position is also present on the P2X$_4$ polypeptide, but not on the other P2X isoforms. Second, from the four *N*-glycans that are cotranslationally attached per P2X$_1$ subunit, only that at Asn^{300} (N5) acquires complex-type carbohydrates during passage of the Golgi apparatus, whereas the others remain in an Endo H-sensitive form. This observation can best be reconciled with constraints imposed by the three-dimensional structure of the P2X$_1$ receptor, which apparently restricts the access of individual *N*-glycans to processing by Golgi enzymes. We considered that the restricted accessibility of the *N*-glycans results from a lectin-like subunit interaction. However, present findings exclude this possibility, since a P2X$_1$ triple mutant devoid of the three inaccessible *N*-glycans (ΔN123) acquired the same homotrimeric configuration like the correctly glycosylated parent P2X$_1$ receptor and formed a functional P2X$_1$ receptor at the plasma membrane, although with low efficiency.

N-Glycans and Membrane Folding of P2X$_1$—The two-dimensional orientation of P2X subunits in the plasma membrane has been predicted from hydropathy plots, usage of natural *N*-glycosylation sites (9), and *N*-glycan scanning mutagenesis studies (38, 39). The five putative *N*-glycosylation sites of the P2X$_1$ polypeptide are all located in the predicted ectodomain. As noted previously, the demonstration that four of the five natural sites are occupied by sugars confirms the membrane topology deduced from hydropathy analysis, since *N*-glycosylation sites occur always on the extracellular portion of a protein. Additional important information about membrane folding can be deduced from the observation that Asn^{300} (N5) is not only used, but also fully accessible to Golgi enzymes to acquire complex-type carbohydrates. N5 is located only eight residues

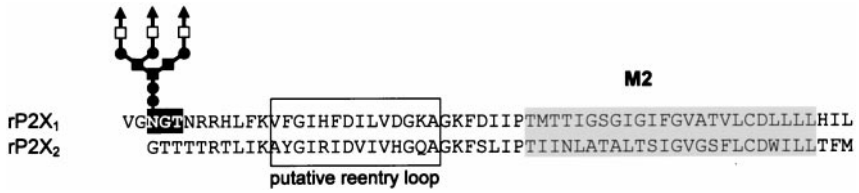

FIG. 6. **Position of complex-glycosylated *N*-glycan of P2X$_1$ relative to a postulated reentry loop.** Amino acid alignment of rat P2X$_1$ and P2X$_2$, including sequon N^{300}GT of P2X$_1$ (*highlighted* in *black*) and the putative second transmembrane domain (M2, *highlighted* in *gray*). The present study demonstrates that N^{300}GT is used as a glycosyl acceptor site and is the only one out of a total of four *N*-glycans that acquires complex-type carbohydrates. The lipophilic sequence AYGIRIDVIVHGQA of rat P2X$_2$ that has been suggested to form a reentry loop (2) and the corresponding sequence of rat P2X$_1$ are *boxed*.

upstream of the conserved lipophilic domain (Fig. 6), which has been postulated to constitute a reentry loop immediately before M2 like the H5 domain of K^+ channels and hence to contribute to the pore (2). Using a cell-free translation system, it has been demonstrated that oligosaccharide transfer occurs only when 12–14 amino acids downstream to a sequon have been translocated (40). The efficient *N*-glycosylation of N5 and its ready accessibility for Golgi enzymes, *i.e.* within the fully assembled P2X$_1$ receptor argue against a significant membrane embedding of this lipophilic domain. The glycan may serve to shield a hydrophobic surface at this locus.

Positional Effects of N-Glycans on Surface Expression of P2X$_1$ Receptor Protein—The most proximal glycan (N1) appears to be especially important for high surface expression levels of functional P2X$_1$ receptors, whereas N2 and N5 are dispensable in this respect. The surprising observation that the expression level of functional receptors increased upon elimination of N3 may be correlated with an increased number of P2X$_1$ receptors at the plasma membrane, as evident from most though not all surface radioiodination experiments (results not shown), rather than by altered receptor function. The mechanism of this increase is not clear yet. The peculiar role of the glycan at N3 for ATP potency is discussed below.

If the modulatory roles of individual *N*-glycans are neglected, it becomes obvious that the elimination of two of the four canonical *N*-glycosylation sites per subunit is quite well tolerated. This suggests that the number of *N*-glycans per P2X$_1$ subunit is redundant, at least for robust expression. A large decline of the expression level occurs only after elimination of three sites per subunit both in terms of maximum current amplitudes and receptor protein at the cell surface. Taking the trimeric architecture of P2X receptors into account, this means that a total of six *N*-glycans are required per receptor complex for robust functional expression. A reduction of surface appearance has been observed for the nonglycosylated forms of a large variety of glycoproteins, but the mechanisms that account for this phenomenon appear to be different. Many nonglycosylated forms of glycoproteins accumulate in the ER, aggregate, and do not exit (41). Others exit the ER, but are retained in the Golgi apparatus, apparently because *N*-linked oligosaccharides are required for efficient transport from the Golgi apparatus to the cell surface (42). Since nonglycosylated His-P2X$_1$ receptor subunits or complexes accumulate neither in the ER nor in the Golgi apparatus, rapid degradation soon after synthesis is likely to account for the low functional expression levels and low amounts of receptor protein at the cell surface of mutants carrying solely one *N*-glycan.

Elimination of all four glycosyl acceptor sites abolished the appearance of His-P2X$_1$ at the cell surface. An essential role of *N*-glycans has been also described for the formation of functional P2X$_2$ receptors in HEK293 cells (43). This raises the possibility that interaction with lectin-like chaperones such as calnexin and/or calreticulin (23) is crucial at certain stages of the folding process and for oligomerization of P2X subunits, for instance by providing additional time to allow for productive collisions between P2X monomers. Incompletely folded monomers that lack *N*-glycans as functional tags may no longer be retained in the ER and eventually get degraded (44).

Conservation of N-Glycosylation Sites among P2X Isoforms—The four *N*-glycans of P2X$_1$ are distributed over two-thirds of the ectodomain like the ten cysteine residues that are assumed to be involved in disulfide formation (Fig. 1). In contrast to the cysteines, however, which are totally conserved among all P2X isoforms, only P2X$_3$ exhibits a *N*-glycan distribution that overlaps exactly with that of P2X$_1$. Sequons corresponding to N1 and N2 of P2X$_1$ are present on almost all isoforms, whereas the sequon corresponding to N5 (Asn^{300}) is found on P2X$_1$-P2X$_3$ only. The number of *N*-glycosylation sites likely to be used amount to three (P2X$_2$, P2X$_5$, P2X$_6$), four (P2X$_1$, P2X$_3$), six (P2X$_7$) and seven (P2X$_4$), *i.e.* all isoforms carry at least three *N*-glycans. Since only two such sites are actually required for robust receptor formation, and no particular *N*-glycan is absolutely important, variation in acceptable positions of glycans can occur. Hence, the redundancy in the number of *N*-glycans provides at least a partial explanation for the imperfect conservation of the number and positions of *N*-glycans among the P2X isoforms.

N-Glycans and Ligand Recognition—Elimination of *N*-glycans has only occasionally been observed to be associated with altered ligand recognition. Lack of *N*-glycosylation of the glucose transporter GLUT1 decreased its apparent affinity for glucose (45). In contrast, the nonglycosylated transporter for serotonin (46) or norepinephrine (47), like the Na^+/glucose symporter SGLT1 (48), exhibited no alteration of substrate recognition. Elimination of the four *N*-glycosylation sites of the insulin receptor β subunit also did not affect the affinity for insulin, but blocked signal transduction (49). The single *N*-glycan of the human T-cell surface glycoprotein CD2 was first suggested by cell adhesion assays to be required for binding of the counter receptor CD58. However, structure resolution by NMR revealed that this *N*-glycan is not directly involved in ligand binding, but crucial for the stabilization of the folded protein structure (50). Presence of a glycan in the vicinity of the α-bungarotoxin binding surface has been demonstrated to confer α-bungarotoxin resistance to the nicotinic acetylcholine receptor (51). Most likely, the bulky glycan moiety imposes steric hindrance for toxin binding. Referred to the present work, one would expect a gain of function, *i.e.* an increase in ATP potency, once a bulky *N*-glycan is removed in the vicinity of the ligand binding site. The observation of a decrease in the potency for ATP, *i.e.* a loss of function, makes it more likely that the glycan at Asn^{210} imposes structural alterations, which may act to stabilize a folded domain essential for ATP binding. A contribution of this region to the ATP binding site can be inferred from the recent observation that neutralization of the conserved residues Lys^{190} and Lys^{215} by alanine substitution produced also a slight (2–5-fold) decrease of ATP potency (52).

Acknowledgment—We thank Dr. Günter Lambrecht for helpful comments about the manuscript.

REFERENCES

1. Valera, S., Hussy, N., Evans, R. J., Adami, N., North, R. A., Surprenant, A., and Buell, G. (1994) *Nature* **371,** 516–519
2. Brake, A. J., Wagenbach, M. J., and Julius, D. (1994) *Nature* **371,** 519–523
3. Chen, C. C., Akopian, A. N., Sivilotti, L., Colquhoun, D., Burnstock, G., and Wood, J. N. (1995) *Nature* **377,** 428–431
4. Bo, X. N., Zhang, Y., Nassar, M., Burnstock, G., and Schoepfer, R. (1995) *FEBS Lett.* **375,** 129–133
5. Buell, G., Lewis, C., Collo, G., North, R. A., and Surprenant, A. (1996) *EMBO J.* **15,** 55–62
6. Soto, F., Garcia-Guzman, M., Gomez-Hernandez, J. M., Hollmann, M., Karschin, C., and Stühmer, W. (1996) *Proc. Natl. Acad. Sci. U. S. A.* **93,** 3684–3688
7. Collo, G., North, R. A., Kawashima, E., Merlo-Pich, E., Neidhart, S., Surprenant, A., and Buell, G. (1996) *J. Neurosci.* **16,** 2495–2507
8. Surprenant, A., Rassendren, F., Kawashima, E., North, R. A., and Buell, G. (1996) *Science* **272,** 735–738
9. Nicke, A., Bäumert, H. G., Rettinger, J., Eichele, A., Lambrecht, G., Mutschler, E., and Schmalzing, G. (1998) *EMBO J.* **17,** 3016–3028
10. Stoop, R., Thomas, S., Rassendren, F., Kawashima, E., Buell, G., Surprenant, A., and North, R. A. (1999) *Mol. Pharmacol.* **56,** 973–981
11. Ding, S., and Sachs, F. (1999) *J. Gen. Physiol.* **113,** 695–720
12. Ding, S., and Sachs, F. (2000) *J. Physiol.* (*Lond.*) **522,** 199–214
13. Soto, F., Garcia-Guzman, M., and Stühmer, W. (1997) *J. Membr. Biol.* **160,** 91–100
14. Burnstock, G. (1999) *Prog. Brain Res.* **120,** 3–10
15. North, R. A. (1996) *Semin. Neurosci.* **8,** 187–194
16. Mackenzie, A. B., Surprenant, A., and North, R. A. (1999) *Ann. N. Y. Acad. Sci.* **868,** 716–729
17. Nicke, A., Büttner, C., Eichele, A., Lambrecht, G., and Schmalzing, G. (1999) *Prog. Brain Res.* **120,** 61–80
18. Virginio, C., MacKenzie, A., Rassendren, F. A., North, R. A., and Surprenant, A. (1999) *Nat. Neurosci.* **2,** 315–321
19. Khakh, B. S., Bao, X. R., Labarca, C., and Lester, H. A. (1999) *Nat. Neurosci.* **2,** 322–330
20. Varki, A. (1993) *Glycobiology* **3,** 97–130
21. Dwek, R. A. (1995) *Biochem. Soc. Trans.* **23,** 1–25
22. Goder, V., Bieri, C., and Spiess, M. (1999) *J. Cell Biol.* **147,** 257–266
23. Trombetta, E. S., and Helenius, A. (1998) *Curr. Opin. Struct. Biol.* **8,** 587–592
24. Hebert, D. N., Foellmer, B., and Helenius, A. (1995) *Cell* **81,** 425–433
25. Lapthorn, A. J., Harris, D. C., Littlejohn, A., Lustbader, J. W., Canfield, R. E., Machin, K. J., Morgan, F. J., and Isaacs, N. W. (1994) *Nature* **369,** 455–461
26. Fiedler, K., and Simons, K. (1995) *Cell* **81,** 309–312
27. Sanger, F., Nicklen, S., and Coulson, A. R. (1977) *Proc. Natl. Acad. Sci. U. S. A.* **74,** 5463–5467
28. Schmalzing, G., Gloor, S., Omay, H., Kröner, S., Appelhans, H., and Schwarz, W. (1991) *Biochem. J.* **279,** 329–336
29. Thompson, J. A., Lau, A. L., and Cunningham, D. D. (1987) *Biochemistry* **26,** 743–750
30. Schägger, H., Cramer, W. A., and von Jagow, G. (1994) *Anal. Biochem.* **217,** 220–230
31. Schägger, H., and von Jagow, G. (1991) *Anal. Biochem.* **199,** 223–231
32. Nicke, A., Rettinger, J., Mutschler, E., and Schmalzing, G. (1999) *J. Recept. Signal. Transduct. Res.* **19,** 493–507
33. Griffon, N., Büttner, C., Nicke, A., Kuhse, J., Schmalzing, G., and Betz, H. (1999) *EMBO J.* **18,** 4711–4721
34. Mulryan, K., Gitterman, D. P., Lewis, C. J., Vial, C., Leckie, B. J., Cobb, A. L., Brown, J. E., Conley, E. C., Buell, G., Pritchard, C. A., and Evans, R. J. (2000) *Nature* **403,** 86–89
35. Shakin-Eshleman, S. H., Spitalnik, S. L., and Kasturi, L. (1996) *J. Biol. Chem.* **271,** 6363–6366
36. Gavel, Y., and Von Heijne, G. (1990) *Protein Eng.* **3,** 433–442
37. Bause, E. (1983) *Biochem. J.* **209,** 331–336
38. Newbolt, A., Stoop, R., Virginio, C., Surprenant, A., North, R. A., Buell, G., and Rassendren, F. (1998) *J. Biol. Chem.* **273,** 15177–15182
39. Torres, G. E., Egan, T. M., and Voigt, M. M. (1998) *FEBS Lett.* **425,** 19–23
40. Nilsson, I., and Von Heijne, G. (1993) *J. Biol. Chem.* **268,** 5798–5801
41. Helenius, A. (1994) *Mol. Biol. Cell* **5,** 253–265
42. Gut, A., Kappeler, F., Hyka, N., Balda, M. S., Hauri, H. P., and Matter, K. (1998) *EMBO J.* **17,** 1919–1929
43. Torres, G. E., Egan, T. M., and Voigt, M. M. (1998) *Biochemistry* **37,** 14845–14851
44. Hebert, D. N., Foellmer, B., and Helenius, A. (1996) *EMBO J.* **15,** 2961–2968
45. Asano, T., Takata, K., Katagiri, H., Ishihara, H., Inukai, K., Anai, M., Hirano, H., Yazaki, Y., and Oka, Y. (1993) *FEBS Lett.* **324,** 258–261
46. Tate, C. G., and Blakely, R. D. (1994) *J. Biol. Chem.* **269,** 26303–26310
47. Melikian, H. E., Ramamoorthy, S., Tate, C. G., and Blakely, R. D. (1996) *Mol. Pharmacol.* **50,** 266–276
48. Wu, J. S., and Lever, J. E. (1994) *Biochim. Biophys. Acta* **1192,** 289–292
49. Leconte, I., Auzan, C., Debant, A., Rossi, B., and Clauser, E. (1992) *J. Biol. Chem.* **267,** 17415–17423
50. Wyss, D. F., Choi, J. S., Li, J., Knoppers, M. H., Willis, K. J., Arulanandam, A. R., Smolyar, A., Reinherz, E. L., and Wagner, G. (1995) *Science* **269,** 1273–1278
51. Kreienkamp, H. J., Sine, S. M., Maeda, R. K., and Taylor, P. (1994) *J. Biol. Chem.* **269,** 8108–8114
52. Ennion, S., Hagan, S., and Evans, R. J. (2000) *J. Biol. Chem.* **275,** 29361–29367